QTL mapping in an interspecific sorghum population uncovers plasma-membrane intrinsic proteins as key regulators of salinity tolerance

Ashley N. Hostetler[1], Rajanikanth Govindarajulu[1,2], Jennifer S. Hawkins[1]

West Virginia University[1]
53 Campus Drive
Department of Biology
West Virginia University
Morgantown, WV 26505

Eurofins Lancaster Labs[2]
601 E. Jackson St.
Richmond, VA 23219

Author for correspondence:
Ashley N. Hostetler
53 Campus Drive
Department of Biology
West Virginia University
Morgantown, WV 26505

Keywords – aquaporins, genetic map, plasma-intrinsic proteins, recombinant inbred line, salinity tolerance, *Sorghum bicolor*, *Sorghum propinquum*, stress tolerance index, quantitative trait loci

Abstract

Soil salinity impedes crop production via both osmotic and ionic stress and is an intensifying problem affecting lands used to produce agronomically important crops.. Such stress slows plant growth and disrupts normal metabolic processes, resulting in decreased biomass and increased leaf senescence. Therefore, the ability to maintain biomass in response to salt exposure is indicative of tolerant genotypes. We used a recombinant inbred line (RIL) population derived from an interspecific cross between *Sorghum propinquum* and *Sorghum bicolor* (inbred Tx7000), two genotypes that differ for tolerance to salt exposure, to map regions of the genome associated with salt tolerance. Our high-density genetic map covers the 10 *Sorghum* chromosomes with 1692 segregating markers. Sixteen total quantitative trait loci (QTL) were detected for seven traits in two environmental conditions (control and salt) and when stress tolerance index (STI) values were mapped. Our results uncovered significant enrichment of genes encoding various types of aquaporins within salt specific QTL, the most interesting of which is the plasma-membrane intrinsic protein SbPIP2;6. SbPIP2;6 shares ~85% sequence similarity with *Arabidopsis* PIP2;1, an aquaporin shown to co-transport both water and ions, and for which ion transport is inhibited by calcium, suggesting that it may play a role in sensing and signaling during the salt stress response. The coupling of water and ion transport may also facilitate the use of Na^+ as a cheap compatible solute, reducing the energy needed to maintain osmotic equilibrium. These results indicate that PIPs play a central role in salinity tolerance in sorghum.

Introduction

Saline soils are an intensifying problem that directly affects the production of agriculturally important crops. Soil salinity is an abiotic stressor where soluble ions, such as Na^+ and Cl^-, accumulate in the soil surrounding root rhizospheres. These ions cause a decrease in the soil water potential, making it difficult for plants to absorb water. With salinity affecting more than 6% of the total land and 20% of the irrigated land, it is imperative to identify ways to maintain and increase crop productivity in saline environments in order to meet population demands (Rengasamy, 2006; Food and Agriculture Organization (FAO), 2008, 2009; Hasegawa, 2013; FAO, 2017; Yang *et al.*, 2020). Research over the last 20 years focused on unraveling the key mechanisms of the salt responsive suggests that tolerance is a product of: 1) ion exclusion, which results in the absence of salt ions from the shoot of the plant, 2) tissue tolerance, achieved by the sequestration of ions into specific tissues, cells, and subcellular organelles, and 3) osmotic tolerance (shoot ion-independent tolerance), defined as the ability to maintain water uptake and growth despite lower water potential (Munns & Tester, 2008; Carillo *et al.*, 2011; Fan *et al.*, 2015; Genc *et al.*, 2016; Negrão *et al.*, 2017; Munns *et al.*, 2019).

Salinity stress negatively affects many economically important crops. Sorghum (*Sorghum bicolor* L. Moench), for which some genotypes are naturally drought and salt tolerant (Boursier & Läuchli, 1990; Almodares & Sharif, 2007; Almodares *et al.*, 2007, 2008b,a; Mullet *et al.*, 2014; Fracasso *et al.*, 2016; McCormick *et al.*, 2018; Guo *et al.*, 2018; Henderson *et al.*, 2020), ranks fifth for food, fuel, and feed production after wheat, maize, rice, and barely (Doggett, 1970, 1988). In a recent study, 18 diverse genotypes of *Sorghum bicolor* and four wild relatives were assessed for performance following salt exposure (Henderson *et al.*, 2020). *Sorghum bicolor* genotypes maintained as little as 30% to as much as 95% of their biomass after 12 weeks of salt exposure, and most of the individuals from the landrace durra ranked in the top five genotypes for most tolerant. Further, the most sensitive genotype, in terms of live aboveground biomass production, was *Sorghum propinquum*, which maintained only 5% of its biomass in response to salinity stress. This wide range in biomass retention indicates continuous variation in salinity tolerance and suggests that tolerance is a quantitatively inherited trait.

Quantitative trait loci (QTL) mapping is a powerful tool that enables the association of quantitatively inherited phenotypes to candidate genomic loci (Kearsey, 1998; Lynch & Walsh, 1999; Broman & Sen, 2009). Given recent results that demonstrate variation among sorghum genotypes and their close relatives (Henderson *et al.*, 2020), the recombinant inbred line (RIL) population used in this study (*S. propinquum* by *S. bicolor* (Tx7000 - landrace durra) serves as a valuable resource to dissect the genetic underpinnings of salinity tolerance. Here, we provide a high-density genetic map from 177 $F_{3:5}$ RILs and identify QTL associated with numerous biomass-related traits that are indicative of salinity tolerance, such as dead aboveground biomass, live aboveground biomass, total aboveground biomass, root biomass, total biomass, rank score, and height. From the 16 total QTL identified, four were identified in the salt population, nine were identified from STI values, and three were identified in the control population. Further, nine of the QTL were unique to either salt or STI values, suggesting that genes within these QTL are important in the genetic controls of salt tolerance. Candidate genes within

these QTL include those previously shown to aid in osmotic and ionic stress alleviation through sensing and signaling of ions, and via ion transport. Interestingly, we identified an enrichment of aquaporins in multiple QTL for which homologs in *Arabidopsis* have been shown to act as non-selective cation channels (Agre, 2004; Hachez & Chaumont, 2010; Kourghi *et al.*, 2017), suggesting a central role in ion sensing and transport during the salt response.

Materials and Methods

Plant Material

A recombinant inbred line (RIL) mapping population derived from an interspecific cross of *Sorghum propinquum* (courtesy Dr. William Rooney, Texas A&M University, College Station, TX) and *Sorghum bicolor* (inbred Tx7000, landrace durra) was used to investigate the genetic underpinnings associated with variation in salinity tolerance. The RIL population consists of 177 $F_{3:5}$ lines with 75% (132 RILs) of the individuals being F_5, 18% (31 RILs) of the individuals being F_4, and 7% (14 RILs) of the individuals being F_3. Each line was derived by the single seed descent method (Brim, 1966; Snape & Riggs, 1975).

Experimental Conditions

In a controlled greenhouse room, five seeds of each RIL were sown in 5 cm x 5 cm x 5 cm planting plugs filled with metromix soil. Conditions during germination were: 21°C, 75% humidity, and 4.5 vapor pressure deficit (VPD). During germination, seedlings were misted regularly with non-saline tap water and watered with a 20-10-20 N-P-K fertilizer (J.R. Peters, Inc., Allentown, PA, USA) diluted to 200 mg N L^{-1} every 4th day. Once all plants reached at least the third leaf stage (V3) of development (approximately 32 days post sowing), soil plugs were transplanted into 5 cm x 5 cm x 25 cm treepots (Stuewe and Sons, Tangent, OR, USA) filled with silica sand #4. Growth conditions were: 27°C day/23°C night with 16 h ambient daylight and 75% humidity. Following transplant, seedlings were watered to saturation with non-saline tap water daily for two weeks to provide a period of establishment. All plants were fertilized twice weekly with a 20-10-20 N-P-K fertilizer (J.R. Peters, Inc., Allentown, PA, USA) diluted to 200 mg N L^{-1} for the remainder of the study. Following establishment, three of the five biological replicates were randomly assigned to a 75 mM NaCl salt treatment and two of the five biological replicates were randomly assigned to a 0 mM NaCl control treatment. Seedlings were watered once daily, in accordance with their assignment, to complete saturation for the duration of the experiment. Treatment began 51 days after planting and plants were treated for a total of 45 days.

Phenotypic Measurements

The following measurements were recorded at various developmental stages for each of the 177 lines: height (cm), tiller count, rank score, root biomass (g), dead aboveground biomass (g), live aboveground biomass (g), total aboveground biomass (g), total biomass (g), and the shoot to root ratio. Height was taken from the base of the stem to the tip of

the newest emerged leaf. Tiller count was the total number of tillers attached to the base of the stem. Rank score was a qualitative score that described overall leaf 'greenness', leaf health, and mortality, where plants that displayed no signs of stress received a low rank score, and plants that were extremely stressed or had died received a high rank score (**Table 1**). Rank score was assessed by the same person throughout the entirety of study to minimize bias. All biomass measurements were taken on tissue collected from a destructive harvest and dried in 65°C for a minimum of 72 h. Root biomass was the total belowground biomass collected. Roots were rinsed in water to remove all dirt and sand. Dead aboveground biomass included all biomass (leaves, tillers, and/or stem) attached to the plant where more than 50% of the tissue was brown; whereas, live aboveground biomass included all biomass attached to the plant that was more than 50% green suggesting it was alive. Total aboveground biomass was the sum of live and dead aboveground biomass, while total biomass included live, dead, and root biomass. The shoot to root ratio was the total aboveground biomass divided by the root biomass. Mortality was scored as 1 if plants were alive and 0 if dead.

Phenotypes were measured at three time points: 0 days (51 days after planting, 0 days of treatment, referred to as pre-treatment), then 15 (short term exposure), and 45 (long term exposure) days after treatment began. Height and tiller count were taken at 0, 15, and 45 days after treatment began, with 0 days indicating immediately before treatment. Rank score was taken at 15 and 45 days after treatment began. All biomass was collected between 45-50 days after treatment and was immediately dried.

The stress tolerance index (STI) value for each trait was calculated using the following formula, where Y is the phenotypic trait, control is the trait measurement in 0 mM NaCl conditions, salt is the trait measurement in 75 mM NaCl conditions, and control average is the population average of the trait in control conditions (Negrão *et al.*, 2017):

$$Stress\ Tolerance\ Index\ = \left(\frac{Ycontrol}{Y\ control\ average}\right) \times \left(\frac{Ysalt}{Y\ control\ average}\right)$$

For each RIL, the control value was averaged across control replicates and an STI value was calculated for each salt treated plant. The STI value accounts for the overall performance of the population and compares each RIL's ability to maintain performance under stress conditions. RILs with large STI values indicate larger phenotypic values for a given trait, and are often considered tolerant depending on the phenotype.

Statistical analysis of phenotypic values

All statistical analyses were performed on the control population, the salt treated population, and on stress tolerance index (STI) values. Three biological replicates of each RIL in the salt population and two biological replicates of each RIL in the control population were considered for QTL analysis. There were three biological replicates for STI values. Least square means for each phenotype in each population (control, salt, STI) were calculated for each RIL. Normality was assessed using both a Shapiro-Wilk test in RStudio (ver.1.2.5019) and Q-Q plots from the *car* (Fox & Weisberg, 2019) package of R (R Core Team, 2013). Traits that were not normally distributed were transformed

(**Supplementary Table S1**). Transformed values were used in statistical tests and in QTL analysis. Correlations of phenotypes within each treatment (control or salt) were assessed via a Pearson's Correlation analysis in R (R Core Team, 2013) using the *PerformanceAnalytics* (Peterson & Carl, 2019) package (**Figure S1**)(R Core Team, 2013).

To determine if there was a treatment effect, both a nonmetric multidimensional scaling (NMDS) analysis (Julkowska *et al.*, 2019) and an analysis of variance (ANOVA) was performed. The NMDS ordination clustered individuals based on Bray–Curtis dissimilarity measures when all phenotypes were considered. The dimcheckMDS function in the *geoveg* package was used to generate stress values for each dimension; two dimensions was deemed appropriate. The NMDS was generated using the *vegan* (Oksanen *et al.*, 2019) package in RStudio (ver.1.2.5019) (R Core Team, 2013). The NMDS was paired with an analysis of similarity (ANOSIM) to statistically test the ordination results from the NMDS. Here, we tested if RILs were more similar within or between treatments (significance assessed at $\alpha = 0.05$). An analysis of variance (ANOVA) was used to test if control and salt populations differed for individual phenotypes (significance assessed at $\alpha = 0.05$). All statistics were completed using RStudio ver.1.2.5019.

Genetic Map Construction and QTL analysis

A high-quality genetic map for the *S. propinquum* by *S. bicolor* (Tx7000) RIL population was previously constructed as described in Govindarajulu *et al.* (2020). In summary, using high-quality nuclear DNA, the parent plants (*S. propinquum* and *S. bicolor*) were sequenced at 18x depth, while the RILs were sequenced at 2x depth. SNP data were aligned to the masked *Sorghum bicolor* reference genome ver 3.1 (Paterson, 2008). Loci were called as *S. propinquum* (A), *S. bicolor* (B), or *heterozygous* (H) when SNPs were analyzed with the GenosToABHPlugin in Tassel ver 5.0 (Bradbury *et al.*, 2007). The ABH formatted SNP data file was then used as input to SNPbinner (Gonda *et al.*, 2019), which calculated breakpoints (Govindarajulu *et al.*, 2020). Breakpoints were merged if they were shorter than 0.2% of the chromosome length. After removing heterozygous bin markers, duplicate bin markers, and markers that deviated significantly from the expected Mendelian ratio (1:1) at $P < 10^{-5}$ after Bonferroni correction, the kosambi map function in R/qtl (Broman *et al.*, 2003) was used to construct a high density genetic map. A second map was constructed including all markers that deviated from the expected Mendelian ratio (1:1).

QTL analysis was performed in RStudio (ver.1.2.5019) using the *qtl* (Broman *et al.*, 2003) package. QTL were first identified by a single interval mapping QTL model. Significant LOD peak scores were determined by comparing LOD peak scores after a 1,000 permutation test ($\alpha = 0.05$) (Churchill & Doerge, 1994). If QTL were detected by interval mapping (IM), phenotypes were assessed via a multiple QTL model. The multiple QTL model (MQM) tested for additional additive QTL, refined QTL positions, and tested for epistasis. Following MQM, a type III analysis of variance assessed the significance of fit for the final model, the proportion of variance explained, and the additive effect. QTL with a negative additive value indicated that the trait was negatively

influenced by *S. bicolor* alleles, whereas a positive additive value indicated that the trait was positively influenced by *S. bicolor* alleles. Genes (*Sorghum bicolor* ver. 3.1) within a 1.0 logarithm of the odds (LOD) confidence interval for each QTL were identified.

Aquaporin Enrichment Analysis

To determine if there was an enrichment of aquaporin genes (SbAQP) located within detected QTL, we randomly sampled the *Sorghum bicolor* (ver 3.1) genome 50 times in RStudio (ver.1.2.5019) (R Core Team, 2013). Starting positions were determined by first randomly selecting a chromosome followed by selecting a random starting position on that chromosome. Chromosome selection was determined by multiplying the total number of chromosomes (2n = 10) by a randomly generated number [runif(1)] between 0 and 1. The resulting number was truncated to an integer and represented the starting chromosome number. This same process was repeated to determine the starting location on the chromosome; however, instead of multiplying a random number by the total number of chromosomes, the random number (between 0 and 1) was multiplied by the size of the corresponding chromosome. The result was again truncated and represented the starting location in the genome (in Mb). Genes within a 5 Mb window (5 Mb downstream from the starting location) were extracted (*Sorghum bicolor* ver 3.1)

Results

High density genetic map

The resequencing, SNP calling, and bin calling of the 177 RILs generated 4055 total bin markers (**Figure S2**). After removing distorted markers (**Figure S3**) and duplicate markers (**Figure S4**), the map covered the 10 *Sorghum* chromosomes with 1692 markers (**Supplementary Table S2**) and was 888.7 cM in length (**Supplementary Table S3**). Chromosomes 7 and 8 contained no distorted regions and chromosomes 3 and 9 contained less than 10 distorted markers. The distorted region of 61.09 Mb to 70.23 Mb on chromosome 2 and the distorted region of 6.37 Mb to 59.45 Mb on chromosome 5 indicate preferential transmission bias of *S. propinquum alleles*. Chromosomes 1, 4, 6, and 10 contain distorted regions favoring *S. bicolor* alleles (**Supplementary Table S3**).

Treatment Effect

The control and salt population summary statistics of phenotypes are listed in **Supplementary Table S4**. With the exception of mortality, all other phenotypes were significantly different between control and salt treated populations (in both short term and long term exposure)(**Supplementary Table S5**). In response to salt exposure, plants were shorter (**Figure 1a**) and had less live aboveground biomass, root biomass, total aboveground biomass, total biomass, and percent of alive aboveground biomass (**Figure 1b**), but had larger rank scores, more dead aboveground biomass, and larger shoot to root ratios (**Figure 1b**). These significant differences between treatment and control conditions, in addition to the clear and significant clustering ($p < 0.001$, ANOSIM

R=0.16) of treatments in the NMDS analysis (**Figure 2**), are indicative of a decrease in performance in response to treatment.

QTL Results and Phenotypic Responses

Although variation among the control and salt population was observed in response to treatment, no QTL were detected for short term salt exposure (DAT=15). Therefore, the remaining analyses focused on QTL detected for long-term salt exposure (DAT=45). All genes detected in QTL when only considering Mendelian segregating markers are listed in **Supplementary Table S6**. Genes detected in QTL when including all markers are listed in **Supplementary Table S7**.

Total biomass (TB)

In control conditions, plants ranged from 1.98 g to 12.18 g of total biomass, with a mean of 7.49 g; however, in salt conditions, an average 32% decrease in total biomass was observed (0.66 g - 9.42 g with a mean of 5.11 g, **Supplementary Table S4**). When considering only Mendelian markers, three QTL were detected, with a common QTL detected on chromosome 4 in both salt conditions and when STI values were mapped (qTB45_4.S and qTB45_4.STI, respectively) (**Figure 3a**). An additional unique QTL was detected on chromosome 5 in the salt population (qTB45_5.S). Each QTL had a positive additive effect indicating that *S. bicolor* alleles positively influenced the total biomass and explained greater than 10 percent of the phenotypic variation. The QTL on chromosome 4 that was detected when STI values were mapped (qTB45_4.STI) explained the greatest amount of phenotypic variation (PVE = 13.02) (**Table 2**). Of the 595 genes within qTB45_4.STI, candidate genes were associated with aquaporins, oxidative stress, salt tolerance, LEA (late embryogenesis abundant) proteins, and transporters (**Supplementary Table S8**). When including distorted markers, the peaks for the two QTL detected on chromosome 4 (qTB45_4S and qTB45_4STI) were not affected (**Supplementary Table S9, Figure 3b**).

Total aboveground biomass (TAGB)

In control conditions, plants accumulated an average of 5.00 g of total aboveground biomass (1.34 g - 8.56 g); however, in response to salt treatment, there was an average 20% decrease in total aboveground biomass (average = 3.98 g) (**Supplementary Table S5**). A single QTL (qTAGB45_4.STI) was detected when STI values were mapped (**Figure 3a**). The QTL was located on chromosome 4 from 62.17 Mb - 66.68 Mb with a peak at 62.29 Mb (**Table 2**). qTAGB45_4.STI explained 12.34 percent of the phenotypic variation and had a positive additive effect, indicating that *S. bicolor* alleles positively influence the total amount of aboveground biomass. qTAGB45_4.STI co-localized with qTB45_5.S and qTB45_4.STI. Therefore, the same 595 total genes and candidate genes identified in the total biomass QTL were also identified for total aboveground biomass. When including distorted markers, the QTL detected on chromosome 4 f remained at approximately the same location; however, an additional QTL was detected for the salt population, explaining 9.49 percent of the phenotypic variation and having a larger additive effect of 0.40 (**Figure 3b**).

Dead aboveground biomass (DAGB)

In control conditions, dead aboveground biomass ranged from 0.06 g to 1.61 g (mean of 0.55 g), whereas in salt conditions there was an average increase of 45% with a mean of 0.80 g (**Supplementary Table S4**). Two QTL (qDAGB45_2.C and qDAGB45_2.STI) were detected on chromosome 2 when control and STI values were mapped (**Figure 3a**) and explained 9.14 and 12.03 percent of the phenotypic variation, respectively (**Table 2**). RILs with *S. propinquum* alleles positively influenced the amount of dead aboveground biomass. In qDAGB45_2.STI, there were 739 genes, including candidates that encode aquaporins, Na^+/H^+ transporters, LEA-like proteins, and CLB (calcium-dependent lipid-binding) proteins (**Supplementary Table S8**). When including all distorted markers an additional QTL was detected on chromosome 9 in the control population. The range of the QTL detected on chromosome 2 when control values were mapped (qDAGB45_2.C) shifted and decreased significantly when distorted markers were included (64.40 Mb - 67.54 Mb, peak @ 65.42); however, when STI values were mapped the QTL peak shifted and the range increased (13.85 Mb - 67.54 Mb, peak @ 62.28 Mb) (**Figure 3b**). The new QTL, qDAGB45_9.C, was detected from 55.47 - 57.91 Mb with a peak at 56.32 Mb and explained 9.71 percent of the phenotypic variation with an additive effect of -0.06.

Live aboveground biomass (LAGB)

In control conditions, live aboveground biomass ranged from 1.20 g to 6.95 g with an average of 4.45 g (**Supplementary Table S4**). In response to salt treatment, there was an average decrease of 28% in live aboveground biomass with a range from 0.32 g to 6.22 g and an average of 3.18 g (**Figure 1b**). Two QTL were detected (qLAGB45_4.STI and qLAGB45_5.STI) when STI values were mapped (**Figure 3a**). Both QTL had positive additive effects, indicating that *S. bicolor* alleles positively influenced live aboveground biomass. The QTL detected on chromosome 4 explained 15.35 percent of the phenotypic variation and the QTL detected on chromosome 5 explained 10.40 percent of the phenotypic variation (**Table 2**). Within qLAGB45_4.STI, there were 577 genes, including genes associated with aquaporins, stress induced proteins, cation efflux proteins, and a calcineurin B subunit protein. Within qLAGB45_5.STI, there were 1356 genes, including genes that encode proteins associated with photosynthesis, auxin signaling and response, stress response, potassium channels, and growth regulation (**Supplementary Table S8**). When distorted markers were included, the QTL on chromosome 4 (qLAGB45_4.STI) was still detectable, but with a slight shift in the range and peak (**Supplementary Table S9**).

Root biomass (RB)

Root biomass for plants grown in control conditions ranged from 0.48 g to 6.38 g with a population average of 2.50 g; however, in salt conditions, root biomass was reduced by an average of 55% and ranged from 0.09 g to 2.48 g with a population average of 1.13 g (**Supplementary Table S4**). A single QTL was detected when STI values were mapped (qRB45_4.STI) (**Figure 3a**). qRB45_4.STI explained 9.09 percent of the phenotypic variation and had an additive effect of 0.08 indicating that individuals with *S. bicolor* alleles in this region positively influenced root biomass. Of the 812 genes within qRB45_4.STI (**Supplementary Table S6**), there were several known for their role in

stress response, specifically genes that have been annotated as salt tolerance homologs (**Supplementary Table S8**). When including all distorted markers, the QTL detected on chromosome 4 was retained in approximately the same location (peak @ 62.46 Mb); however, the range of the QTL was reduced (62.17 Mb - 62.54 Mb)(**Figure 3b**).

Rank score (RS)

Rank score was a qualitative measure used to describe overall plant health (**Table 1**). There was an average 58% increase in rank score in response to treatment, indicating that there was an overall decrease in the health of plants exposed to NaCl (**Figure 1b**). In control conditions, the average rank score of the population was 2.01 (0.72-3.20) indicating that most of the individuals in the population were beginning to show signs of leaf tip curling; however, some individuals had dead leaves present but still were able to produce new leaves. In contrast, the rank score of the salt treated population averaged 3.19 with a range of 1.68 to 4.55 (**Supplementary Table S4**). This increase suggests that the production of new leaves was halted, most leaves were dead or began dying, and all individuals were displaying signs of stress. When STI values were mapped, a single QTL (qRS45_7.STI) was detected on chromosome 7 (**Figure 3a**). qRS45_7.STI explained 9.00 percent of the phenotypic variation and had a negative additive effect indicating that *S. bicolor* alleles are associated with a lower the rank score. Of the 134 genes located within qRS45_7.STI, there are genes that encode aquaporins and cation transporters (**Supplementary Table S8**). When all distorted markers were included a new QTL was detected on chromosome 4 (qRS45_4.STI). qRS45_4.STI ranged from 62.46 Mb - 63.95 Mb with a peak near 63.67 Mb (**Figure 3b**). qRS45_4.STI explained 10.77 percent of the phenotypic variation and also had a negative additive effect of 0.19, indicating that *S. bicolor* alleles are associated with overall better plant health in stress conditions.

Height (HT)

At the final recording of height, the control population ranged from 52.92 cm to 122.37 cm with a population average of 87.81 cm. In response to treatment, the salt population displayed an average of 16.38% decrease in height, ranging from 46.32 cm to 112.47 cm with a population average of 75.46 cm (**Figure 1a**). Six QTL were detected for height with two common QTL in the control (qHT45_7.C and qHT45_9.C) population and when STI values were mapped (qHT45_7.STI and qHT45_9.STI) (**Table 2**). qHT45_7.S was also detected in the salt population; however, an additional unique QTL (qHT45_1.S) was detected in the salt population, explaining 12.07 percent of the phenotypic variation and having an additive effect of -4.36. Of the 3644 total genes within qHT45_1.S, several candidate genes were identified, including genes associated with osmotic and ionic stress alleviation, such as SOS3- and CBL-interacting proteins, and vacuolar cation exchangers (**Supplementary Table S8**). When including distorted markers, all six previously detected QTL remained; however, an additional two QTL were detected when STI values were mapped (**Figure 3b**). With the exception of qHT45_1.S, the positions of all other QTL (qHT45_7.C, qHT45_9.C, qHT45_7.S, qHT45_7.STI, and qHT45_9.STI) were unchanged. The range of qHT45_1.S decreased (76.22 Mb to 80.57 Mb); however, the peak remained close to its original location in the Mendelian map (peak @ 75.72 Mb). The two additional QTL detected when STI values

were mapped (qHT45_1.STI and qHT45_4.STI) explained an average 9.82 percent of the phenotypic variation. Interestingly, qHT45_1.STI had a negative additive effect indicating that *S. bicolor* alleles negatively influenced plant height while qHT45_4.STI had a positive additive effect indicating that *S. bicolor* alleles positively influenced height. Further, qHT45_1.STI co-localized with the previously detected qHT45_1.S, which was only detected when salt values were mapped.

Enrichment Analysis

A total of 11,131 genes were located within 1.0 logarithm of the odds (LOD) confidence interval of all QTL identified in this study (**Table 2**, **Supplementary Table S6**). Of these 11,131 total genes, we identified 29 genes that encode aquaporins, with 18 of the 29 genes unique to salt/STI specific QTL. In order to determine if this constitutes an enrichment of aquaporin genes, we performed a random sampling of 50 independent 5 Mb segments (34% of the genome) from the *S. bicolo*r reference genome and recorded the number of aquaporins found in each segment. A total of 9098 genes were identified, of which only 9 encode aquaporins, suggesting an enrichment of aquaporins in the salt QTL that cannot be explained by random chance.

Discussion

In the present study, we screened 177 $F_{3:5}$ RILs derived from a cross between the inbred *Sorghum bicolor* (Tx7000; landrace durra) and its wild relative, *Sorghum propinquum,* for performance-related traits in saline conditions. Because of Sorghum's importance in biofuel and forage production, salinity tolerance was assessed as the ability of the plant to maintain traits related to growth and performance in response to salt treatment. This tolerance can be achieved by various mechanisms including osmotic adjustment, Na^+ exclusion from the aerial organs of the plant, and overall tissue tolerance; however, Na^+ exclusion can also result from reduced Na^+ uptake, increased Na^+ extrusion to the roots and/or soil media, or increased retrieval from the shoot (Wu *et al.*, 2019). Ultimately, each of these tolerance mechanisms results in the maintenance of plant vigor similar to those plants grown in optimal conditions. In this study, we identified QTL associated with total biomass, total aboveground biomass, height, dead aboveground biomass, live aboveground biomass, root biomass, and rank score, in a control environment, a saline environment, and from STI values. Among the 16 QTL detected, 10 were either 1) unique to the STI values, 2) unique to the saline environment, and/or 3) explained more than 10 percent of the phenotypic variation (**Table 2**).

The data presented here, in combination with previous findings (Henderson *et al.* 2020), collectively demonstrates that there is increased tolerance to salinity stress in *S. bicolor* compared to *S. propinquum*. For dead aboveground biomass, live aboveground biomass, total aboveground biomass, and total biomass, *S. bicolor* alleles were associated with tolerance. For example, the negative additive effect for the QTL detected for dead aboveground biomass indicates that *S. bicolor* alleles were associated with less accumulation of dead aboveground biomass. Similarly, the QTL detected for live aboveground biomass, total aboveground biomass, and total biomass all have positive additive effects indicating that *S. bicolor* alleles promote continued growth in stressful

conditions. It is important to note that, in optimal conditions, *S. propinquum* produces more aboveground biomass compared to *S. bicolor* (Govindarajulu *et al.*, 2020). Therefore, in response to salt, the ability for lines with *S. bicolor* alleles to perform favorably supports the conclusion that *S. bicolor* possesses greater tolerance to salinity stress. Further, these results suggest that *S. bicolor* is better at handling both osmotic and ionic stress, because with osmotic adjustment, increased water can be taken up by the plant to support the production of new biomass and to limit necrosis due to cell dehydration, while increased ionic tolerance results in decreased leaf senescence resulting in overall greater aboveground growth.

Because salinity stress is the product of both osmotic and ionic factors, their respective causes and consequences are often difficult to disentangle; however, these two stresses are often temporal in their action. When salts initially begin to accumulate in the soil, the osmotic potential of the soil water decreases, resulting in decreased water extraction by plant roots. This osmotic stress causes a sudden, short term loss of water, cell volume, and turgor from leaf cells. Plants that are tolerant to stress during the osmotic phase are better able to modify long distance signaling, limit stomatal closure, osmotically adjust, and continue cell expansion/lateral bud development, resulting in the continuation of both above and belowground growth (Munns & Tester, 2008). One important mechanism that plants utilize to overcome the osmotic phase of salinity stress is the production and accumulation of compatible solutes such as amino acids (i.e. proline), amines, betaines, organic acids, sugars, and polyols (Parihar *et al.*, 2015), which aid in water acquisition and maintenance of cell turgor. For the QTL detected in this study, we identified various genes whose products are related to osmotic adjustment, including genes involved in proline production, aquaporins, CDPKs (calcium-dependent protein kinases), sensing and signaling, cell division, Na^+/Ca^{2+} exchanger, leaf senescence, early response to dehydration, heat shock proteins, SAPK3 (stress-activated protein kinases), vacuolar proton exchangers, potassium antiporters, and stress response proteins.

Following osmotic stress, as soil salinity levels rise, plants begin to accumulate Na^+ and Cl^- ions, which if not properly handled will become toxic within the leaves. The most common phenotype associated with ionic stress is increased leaf necrosis. Therefore, we used dead aboveground biomass and rank score as a proxy for ionic toxicity. RILs with greater amounts of dead aboveground biomass or larger rank scores were considered sensitive to ionic stress, whereas tolerant genotypes exhibit less leaf necrosis. For qDAGB45_2.STI, *S. propinquum* alleles positively correlated with greater dead aboveground biomass, possibly as a result of increased Na^+ accumulation in the aerial plant tissue. Larger amounts of dead aboveground biomass are often a result of the inability to exclude ions resulting in toxic accumulation, ionic disequilibrium, or tissue sensitivity (Munns & Tester, 2008). Similarly, qRS45_7.STI also had a negative additive effect, indicating that *S. propinquum* alleles positively influenced the rank score, suggestive of greater susceptibility to ionic toxicity (**Table 1**). Candidate genes associated with ionic stress in these QTL include: calcium-dependent protein kinases, LEA-like proteins, aquaporins, heat shock proteins, Na^+/H^+ antiporters, WRKY transcription factors, K^+ uptake, and cation transporters (**Supplementary Table S8**). Most interestingly, there were numerous genes within the two QTL that we considered

informative of ionic stress, specifically genes associated with Ca^{2+} sensing/signaling and Na^{+} transport, which are important in limiting cytoplasmic ion toxicity. A notable candidate gene associated with ionic sensing and signaling identified in qDAGB45_2.STI is CDPK (calcium-dependent protein kinase) (Sobic.002G114800). CDPKs are a class of calcium sensors that, in response to most environmental stresses, have been previously shown to mediate abiotic stress via calcium waves that signal various physiological responses (Urao *et al.*, 1994a,b; Knight *et al.*, 1997; Cheng *et al.*, 2002; Delormel & Boudsocq, 2019). Further, two genes that encode Na^{+}/H^{+} transporters were identified as candidate genes. Na^{+}/H^{+} transporters are especially important in sodium exclusion from areas of the plant such as the cytoplasm and aerial organs. Lastly, genes associated with potassium uptake and distribution were identified. Potassium (K^{+}) is an essential nutrient for plant growth and development (Maathuis, 2009; Ahmad & Maathuis, 2014; Morton *et al.*, 2019). Because of the similarity in size and structure of Na^{+} and K^{+}, both ions often share transport systems. K^{+}, however, is essential for protein synthesis (Jones *et al.*, 1979; Blaha *et al.*, 2000), enzymatic reactions (Bhandal & Malik, 1988), and signaling (Shabala, 2017), whereas Na^{+} is not. Therefore, maintaining high K^{+}/Na^{+} ratios is important for salinity tolerance (Chen *et al.*, 2005, 2007; Cuin *et al.*, 2008; Shabala, 2013; Wu *et al.*, 2018; Morton *et al.*, 2019).

We observed an enrichment of genes encoding various types of aquaporins in salt-stress related QTL (**Supplementary Table S6**). Aquaporins are well known for their role in the transport of water and other neutral solutes (Sakurai *et al.*, 2005; Alexandersson *et al.*, 2005; Maurel *et al.*, 2008; Liu *et al.*, 2015; Reddy *et al.*, 2015; Kadam *et al.*, 2017; Hasan *et al.*, 2017). In a previous study that characterized the aquaporin (AQP) gene family in *Sorghum bicolor*, SbAQP transcript abundance was affected by both salt and drought stress (Reddy *et al.*, 2015). In our study we identified 15 unique aquaporin genes, which encode TIP3;1, SIP2;1, PIP2;2, PIP2;6, PIP1;3, PIP1;4, TIP2;1, SIP1;1, and NIP3;2 (**Supplementary Table S6**). When including all markers, a total of 12 unique aquaporin genes were identified, which encode TIP1;1, TIP3;1, PIP2;2, PIP2;6, PIP2;7, PIP1;3, PIP1;4, TIP2;1, and PIP1;5 (**Supplementary Table S7**). While many of the same genes were identified in both genetic maps (**Figure 3**), TIP1;1, and PIP1;5 were present only after including all markers that deviated significantly from the expected 1:1 Mendelian ratio.

Emerging evidence indicates that some aquaporins are also capable of coupling water and ion transport, resulting in osmotic adjustment (Byrt *et al.*, 2017). Specifically, the *Arabidopsis* plasma membrane intrinsic proteins AtPIP2;1 (AT3G53420) and AtPIP2;2 (AT2G37170) have been shown to co-transport water and Na^{+}, suggesting that they play dual roles in nutrient transport and osmotic adjustment (Byrt *et al.*, 2017; Kourghi *et al.*, 2017). In the presence of salts, PIP2 is transported from the plasma membrane, resulting in significant reductions in root hydraulic conductance (Boursiac *et al.*, 2005; Sutka *et al.*, 2011; Byrt *et al.*, 2017). In addition, the ionic conductance of AtPIP2;1 has been shown to be inhibited by divalent cations, specifically Ca^{2+}, which is known to play an essential role in intracellular signalling in plants, particularly in response to abiotic stress (Maurel *et al.*, 2008; Verdoucq *et al.*, 2008; Byrt *et al.*, 2017). Therefore, AtPIP2;1 may constitute a mechanism of sensing and signalling during the salt stress response in plants.

In our study, we identified the tandemly arranged Sobic.002G125000, Sobic.002G125200, Sobic.002G125300, and Sobic.002G125700 which encode copies of SbAQP2;6, lie within the salt-specific QTL qDAGB_2.STI on chromosome 2, and share ~85% sequence similarity with AtPIP2;1 (**Supplementary Table S7**). Given their presence in salt specific QTL, known response to abiotic stress, and high sequence similarity to AtPIP2;1, we propose that these aquaporins play a critical role in maintaining water balance, controlling ion transport, and possibly in sensing and signaling, as mechanisms of salinity tolerance in sorghum.

Conclusions

In our previous study comparing salt tolerance rankings among a diverse group of *Sorghum* genotypes and species, we concluded that the most parsimonious explanation for the phylogenetic distribution of variation in plant response to salinity is that tolerance was acquired early during domestication, specifically in the durra landrace, and then lost in improved lines in a lineage-specific manner (Henderson *et al.*, 2020). Since drought stress and salt stress share a common osmotic component, and since *S. bicolor* was domesticated and improved in arid environments, we hypothesized that the salt tolerance in *Sorghum* is a byproduct of the drought tolerance acquired during domestication. The results presented here, specifically with respect to the enrichment of aquaporins in salt responsive QTL, support the conclusion that the greater salt tolerance in *Sorghum bicolor* is likely a product of efficient water acquisition. In addition to SbPIP2;6, we observed numerous other genes associated with sensing, signaling, and transport of Na^+. Therefore, it is possible that sorghum is also equipped to maintain ionic homeostasis, while facilitating the conservation of energy by using Na^+ as a cheap compatible solute. Sorghum plants would therefore be able to avoid ionic toxicity and alleviate osmotic stress, while also conserving energy that can be used for biomass production (Munns *et al.*, 2019, 2020). The enrichment of AtPIP2;1 homologs within the salt specific QTL, in addition to their previously demonstrated role in water and ion transport in *Arabidopsis*, suggests they play a key role in sensing, signaling, and transport, all of which are critical for increased tolerance. When considering the QTL and candidate genes identified here, we propose that SbPIP2;6 provides a promising avenue of research aimed at the improvement of sorghum for growth on saline soils. Additionally, while there were several other genes identified in this study that have previously been shown to contribute to increased abiotic stress and salinity tolerance, there were a significant number of unannotated genes. These genes remain attractive candidates for future studies, as they may be pivotal in the maintenance of plant health and biomass production in marginal environments.

Acknowledgements

We would like to acknowledge the WVU Genomics Core Facility, Morgantown WV for support provided to help make this publication possible and CTSI Grant #U54 GM104942 which in turn provides financial support to the Core Facility. The authors wish to thank Ryan Percifield for assistance during data collection, Dr. Stephen DiFazio and Dr. Sandra Simon for guidance in data analysis, and the West Virginia University Evansdale Greenhouse for supplying space. This work was partially funded by the Eberly College of Arts and Sciences research award to Ashley N. Hostetler.

Author Contributions

A.N.H and J.S.H designed experiments; A.N.H and J.S.H managed the project; A.N.H., prepared the samples; A.N.H. and R.G. lead the data analysis; A.N.H, and J.S.H wrote the manuscript with contributions from R.G.

References

Agre P. **2004**. Aquaporin water channels (Nobel lecture). *Angewandte Chemie International Edition* **43**: 4278–4290.

Ahmad I, Maathuis FJM. **2014**. Cellular and tissue distribution of potassium: Physiological relevance, mechanisms and regulation. *Journal of Plant Physiology* **171**: 708–714.

Alexandersson E, Fraysse L, Sjövall-Larsen S, Gustavsson S, Fellert M, Karlsson M, Johanson U, Kjellbom P. **2005**. Whole Gene Family Expression and Drought Stress Regulation of Aquaporins. *Plant Molecular Biology* **59**: 469–484.

Almodares A, Hadi MR, Ahmadpour H. **2008a**. Sorghum stem yield and soluble carbohydrates under different salinity levels. *African Journal of Biotechnology* **7**: 4051–4055.

Almodares A, Hadi MR, Dosti B. **2007**. Effects of salt stress on germination percentage and seedling growth in sweet sorghum cultivars. *Journal of Biological Sciences* **7**: 1492–1495.

Almodares A, Hadi MR, Dosti B. **2008b**. The Effects of Salt Stress on Growth Parameters and Carbohydrates Contents in Sweet Sorghum. *Research Journal of Environmental Sciences* **2**: 298–304.

Almodares A, Sharif ME. **2007**. Effects of irrigation water qualities on biomass and sugar contents of sugar beet and sweet sorghum cultivars. : 6.

Bhandal IS, Malik CP. **1988**. Potassium Estimation, Uptake, and Its Role in the Physiology and Metabolism of Flowering Plants. In: Bourne GH, Jeon KW, Friedlander M, eds. International Review of Cytology. Academic Press, 205–254.

Blaha G, Stelzl U, Spahn CMT, Agrawal RK, Frank J, Nierhaus KH. **2000**. Preparation of functional ribosomal complexes and effect of buffer conditions on tRNA positions observed by cryoelectron microscopy. In: Methods in Enzymology. Elsevier, 292–309.

Boursiac Y, Chen S, Luu D-T, Sorieul M, van den Dries N, Maurel C. **2005**. Early Effects of Salinity on Water Transport in Arabidopsis Roots. Molecular and Cellular Features of Aquaporin Expression. *Plant Physiology* **139**: 790–805.

Boursier P, Läuchli A. **1990**. Growth Responses and Mineral Nutrient Relations of Salt-Stressed Sorghum. *Crop Science* **30**: 1226–1233.

Bradbury PJ, Zhang Z, Kroon DE, Casstevens TM, Ramdoss Y, Buckler ES. **2007**. TASSEL: software for association mapping of complex traits in diverse samples. *Bioinformatics* **23**: 2633–2635.

Brim CA. **1966**. A modified pedigree method of selection in soybeans 1. *Crop Science* **6**: 220–220.

Broman KW, Sen Saunak. **2009**. *A guide to QTL mapping with R/qtl*. New York: Springer.

Broman KW, Wu H, Sen S, Churchill GA. **2003**. R/qtl: {QTL} mapping in experimental crosses. *Bioinformatics* **19**: 889–890.

Byrt CS, Zhao M, Kourghi M, Bose J, Henderson SW, Qiu J, Gilliham M, Schultz C, Schwarz M, Ramesh SA, *et al.*2017. Non-selective cation channel activity of aquaporin AtPIP2;1 regulated by Ca2+ and pH. *Plant, Cell & Environment* **40**: 802–815.

Carillo P, Annunziata MG, Pontecorvo G, Fuggi A, Woodrow P. **2011**. Salinity Stress and Salt Tolerance. In: Abiotic Stress in Plants - Mechanisms and Adaptations.

Chen Z, Newman I, Zhou M, Mendham N, Zhang G, Shabala S. **2005**. Screening plants for salt tolerance by measuring K+ flux: a case study for barley. *Plant, Cell & Environment* **28**: 1230–1246.
Chen Z, Pottosin II, Cuin TA, Fuglsang AT, Tester M, Jha D, Zepeda-Jazo I, Zhou M, Palmgren MG, Newman IA, *et al.*2007. Root plasma membrane transporters controlling K+/Na+ homeostasis in salt-stressed barley. *Plant Physiology* **145**: 1714–1725.
Cheng S-H, Willmann MR, Chen H-C, Sheen J. **2002**. Calcium Signaling through Protein Kinases. The Arabidopsis Calcium-Dependent Protein Kinase Gene Family. *Plant Physiology* **129**: 469–485.
Churchill GA, Doerge RW. **1994**. Empirical threshold values for quantitative trait mapping. *Genetics* **138**: 963–971.
Cuin TA, Betts SA, Chalmandrier R, Shabala S. **2008**. A root's ability to retain K^+ correlates with salt tolerance in wheat. *Journal of Experimental Botany* **59**: 2697–2706.
Delormel TY, Boudsocq M. **2019**. Properties and functions of calcium-dependent protein kinases and their relatives in Arabidopsis thaliana. *New Phytologist* **224**: 585–604.
Doggett H. **1970**. Sorghum. *Sorghum.*
Doggett H. **1988**. *Sorghum*. Harlow, Essex, England: Longman Scientific & Technical ;
Fan Y, Shabala S, Ma Y, Xu R, Zhou M. **2015**. Using QTL mapping to investigate the relationships between abiotic stress tolerance (drought and salinity) and agronomic and physiological traits. *BMC Genomics* **16**: 43.
FAO. **2017**. FAO soils portal.
Food and Agriculture Organization (FAO). **2008**. Land and plant nutrition management service.
Food and Agriculture Organization (FAO). **2009**. Land and plant nutrition management service.
Fox J, Weisberg S. **2019**. *An {R} companion to applied regression*. Thousand Oaks, CA: Sage.
Fracasso A, Trindade L, Amaducci S. **2016**. Drought tolerance strategies highlighted by two Sorghum bicolor races in a dry-down experiment. *Journal of Plant Physiology* **190**: 1–14.
Genc Y, Oldach K, Taylor J, Lyons GH. **2016**. Uncoupling of sodium and chloride to assist breeding for salinity tolerance in crops. *New Phytologist* **210**: 145–156.
Gonda I, Ashrafi H, Lyon DA, Strickler SR, Hulse-Kemp AM, Ma Q, Sun H, Stoffel K, Powell AF, Futrell S, *et al.*2019. Sequencing-Based Bin Map Construction of a Tomato Mapping Population, Facilitating High-Resolution Quantitative Trait Loci Detection. *The Plant Genome* **12**: 180010.
Govindarajulu R, Henderson AN, Xiao Y, Chaluvadi SR, Mauro-Herrera M, Siddoway ML, Whipple C, Bennetzen JL, Devos KM, Doust AN, *et al.*2020. Integration of high-density genetic mapping with transcriptome analysis uncovers numerous agronomic QTL and reveals candidate genes for the control of tillering in sorghum. *bioRxiv*: 2020.07.06.189548.
Guo YY, Tian SS, Liu SS, Wang WQ, Sui N. **2018**. Energy dissipation and antioxidant enzyme system protect photosystem II of sweet sorghum under drought stress. *Photosynthetica* **56**: 861–872.

Hachez C, Chaumont F. **2010**. Aquaporins: a family of highly regulated multifunctional channels. In: MIPs and their Role in the Exchange of Metalloids. Springer, 1–17.
Hasan SA, Rabei SH, Nada RM, Abogadallah GM. **2017**. Water use efficiency in the drought-stressed sorghum and maize in relation to expression of aquaporin genes. *Biologia Plantarum* **61**: 127–137.
Hasegawa PM. **2013**. Sodium (Na+) homeostasis and salt tolerance of plants. *Environmental and Experimental Botany* **92**: 19–31.
Henderson AN, Crim PM, Cumming JR, Hawkins JS. **2020**. Phenotypic and physiological responses to salt exposure in Sorghum reveal diversity among domesticated landraces. *American Journal of Botany* **107**: 983–992.
Jones WRG, Brady CJ, Speirs J. **1979**. Ionic and osmotic relations in plant cells. In: Recent advances in cereal biochemistry. London: Academic Press, 63–103.
Julkowska MM, Saade S, Agarwal G, Gao G, Pailles Y, Morton MJL, Awlia M, Tester M. **2019**. MVApp - Multivariate analysis application for streamlined data analysis and curation. *Plant Physiology* **180**: 1261–1276.
Kadam S, Abril A, Dhanapal AP, Koester RP, Vermerris W, Jose S, Fritschi FB. **2017**. Characterization and Regulation of Aquaporin Genes of Sorghum [Sorghum bicolor (L.) Moench] in Response to Waterlogging Stress. *Frontiers in Plant Science* **8**.
Kearsey MJ. **1998**. The principles of QTL analysis (a minimal mathematics approach). **49**: 1619–1623.
Knight H, Trewavas AJ, Knight MR. **1997**. Calcium signalling in Arabidopsis thaliana responding to drought and salinity. *The Plant Journal* **12**: 1067–1078.
Kourghi M, Nourmohammadi S, Pei JV, Qiu J, McGaughey S, Tyerman SD, Byrt CS, Yool AJ. **2017**. Divalent Cations Regulate the Ion Conductance Properties of Diverse Classes of Aquaporins. *International Journal of Molecular Sciences* **18**: 2323.
Liu P, Yin L, Wang S, Zhang M, Deng X, Zhang S, Tanaka K. **2015**. Enhanced root hydraulic conductance by aquaporin regulation accounts for silicon alleviated salt-induced osmotic stress in Sorghum bicolor L. *Environmental and Experimental Botany* **111**: 42–51.
Lynch M, Walsh B. **1999**. Genetics and Analysis of Quantitative Traits. *The Quarterly Review of Biology* **74**: 225–225.
Maathuis FJ. **2009**. Physiological functions of mineral macronutrients. *Current Opinion in Plant Biology* **12**: 250–258.
Maurel C, Verdoucq L, Luu D-T, Santoni V. **2008**. Plant aquaporins: membrane channels with multiple integrated functions. *Annual Review of Plant Biology* **59**: 595–624.
McCormick RF, Truong SK, Sreedasyam A, Jenkins J, Shu S, Sims D, Kennedy M, Amirebrahimi M, Weers BD, McKinley B, *et al.*2018. The Sorghum bicolor reference genome: improved assembly, gene annotations, a transcriptome atlas, and signatures of genome organization. *The Plant Journal* **93**: 338–354.
Morton MJL, Awlia M, Al-Tamimi N, Saade S, Pailles Y, Negrão S, Tester M. **2019**. Salt stress under the scalpel – dissecting the genetics of salt tolerance. *The Plant Journal* **97**: 148–163.
Mullet J, Morishige D, McCormick R, Truong S, Hilley J, McKinley B, Anderson R, Olson SN, Rooney W. **2014**. Energy Sorghum--a genetic model for the design of C4 grass bioenergy crops. *Journal of Experimental Botany* **65**: 3479–3489.

Munns R, Day DA, Fricke W, Watt M, Arsova B, Barkla BJ, Bose J, Byrt CS, Chen Z-H, Foster KJ, *et al.*2020. Energy costs of salt tolerance in crop plants. *New Phytologist*: 1072–1090.
Munns R, Passioura JB, Colmer TD, Byrt CS. **2019**. Osmotic adjustment and energy limitations to plant growth in saline soil. *New Phytologist*.
Munns R, Tester M. **2008**. Mechanisms of salinity tolerance. *Annual Review of Plant Biology* **59**: 651–681.
Negrão S, Schmöckel SM, Tester M. **2017**. Evaluating physiological responses of plants to salinity stress. *Annals of Botany* **119**: 1–11.
Oksanen J, Blanchet FG, Friendly M, Kindt R, Legendre P, McGlinn D, Minchin PR, O'Hara RB, Simpson GL, Soylmos P, *et al.*2019. *vegan: Community Ecology Package*.
Parihar P, Singh S, Singh R, Singh VP, Prasad SM. **2015**. Effect of salinity stress on plants and its tolerance strategies: a review. *Environmental Science and Pollution Research* **22**: 4056–4075.
Paterson AH. **2008**. Genomics of Sorghum. *International Journal of Plant Genomics* **2008**: e362451.
Peterson BG, Carl P. **2019**. *PerformanceAnalytics: Econometric Tools for Performance and Risk Analysis*.
R Core Team. **2013**. *R: A language and enviornment for satistical computing.* Vienna, Austria: R Foundation for Statistical Computing.
Reddy PS, Rao TSRB, Sharma KK, Vadez V. **2015**. Genome-wide identification and characterization of the aquaporin gene family in Sorghum bicolor (L.). *Plant Gene* **1**: 18–28.
Rengasamy P. **2006**. World salinization with emphasis on Australia. *Journal of Experimental Botany* **57**: 1017–1023.
Sakurai J, Ishikawa F, Yamaguchi T, Uemura M, Maeshima M. **2005**. Identification of 33 Rice Aquaporin Genes and Analysis of Their Expression and Function. *Plant and Cell Physiology* **46**: 1568–1577.
Shabala S. **2013**. Learning from halophytes: physiological basis and strategies to improve abiotic stress tolerance in crops. *Annals of Botany*: mct205.
Shabala S. **2017**. Signalling by potassium: another second messenger to add to the list? *Journal of Experimental Botany* **68**: 4003–4007.
Snape JW, Riggs TJ. **1975**. Genetical consequences of single seed descent in the breeding of self-pollinating crops. *Heredity* **35**: 211–219.
Sutka M, Li G, Boudet J, Boursiac Y, Doumas P, Maurel C. **2011**. Natural variation of root hydraulics in Arabidopsis grown in normal and salt-stressed conditions. *Plant physiology* **155**: 1264–1276.
Urao T, Katagiri T, Mizoguchi T, Yamaguchi-Shinozaki K, Hayashida N, Shinozaki K. **1994a**. Two genes that encode Ca2+-dependent protein kinases are induced by drought and high-salt stresses in Arabidopsis thaliana. *Molecular and General Genetics MGG* **244**: 331–340.
Urao T, Katagiri T, Mizoguchi T, Yamaguchi-Shinozaki K, Hayashida N, Shinozaki K. **1994b**. An *Arabidopsis thaliana* cDNA encoding Ca^{2+}-dependent protein kinase. *Plant Physiology* **105**: 1461–1462.
Verdoucq L, Grondin A, Maurel C. **2008**. Structure–function analysis of plant

aquaporin At PIP2; 1 gating by divalent cations and protons. *Biochemical Journal* **415**: 409–416.
Wu H, Shabala L, Zhou M, Su N, Wu Q, Ul-Haq T, Zhu J, Mancuso S, Azzarello E, Shabala S. **2019**. Root vacuolar Na+ sequestration but not exclusion from uptake correlates with barley salt tolerance. *The Plant Journal*: 1–13.
Wu H, Zhang X, Giraldo JP, Shabala S. **2018**. It is not all about sodium: revealing tissue specificity and signalling roles of potassium in plant responses to salt stress. *Plant and Soil* **431**: 1–17.
Yang Z, Li J-L, Liu L-N, Xie Q, Sui N. **2020**. Photosynthetic Regulation Under Salt Stress and Salt-Tolerance Mechanism of Sweet Sorghum. *Frontiers in Plant Science* **10**.

Figure Legends

Figure 1. Phenotypic averages in control (0 mM NaCl) and treatment (75 mM NaCl) conditions. (A) Phenotype averages for the control population and the salt population for height (HT) (cm). The x-axis shows the days after treatment and the y-axis describes the height in cm. (B) Phenotypic averages for the control population and salt population for dead aboveground biomass (DAGB) (g), live aboveground biomass (LAGB) (g), mortality, root biomass (RB) (g), rank score (RS) (0-5), shoot to root ratio (SRR), total aboveground biomass (TAGB) (g), total biomass (TB) (g), and tiller number (TN). In response to salt exposure, dead aboveground biomass, rank score, and shoot to root ratio increased, whereas height, live aboveground biomass, root biomass, total aboveground biomass, and total biomass decreased. The x-axis lists the phenotype of interest and the y-axis represents the population average for each phenotype.

Figure 2. Non-metric multidimensional scaling (NMDS) analysis paired with an analysis of similarity (ANOSIM) reveals treatment clustering. A NMDS paired with an ANOSIM reveals that individuals were more similar within a treatment than between treatments (ANOSIM $R=0.16$, $p<0.001$).

Figure 3. Sorghum genetic map with QTL locations for 14 traits from $177_{F3:F5}$ RILs. (A) QTL detected from a high-density genetic map using only Mendelian (non-distorted) segregating markers. Markers were considered distorted at $p < 10\text{-}5$ after Bonferroni correction. Empty regions are regions that were removed because bins were either heterozygous, distorted, or were duplicates. *Note: the genetic distance on chromosome 6 is inflated due to segregation distortion. (B) QTL detected from a high-density genetic map that includes markers that deviated significantly from the Mendelian ratio (1:1). Empty spaces are regions that were removed because bins were either heterozygous or duplicate markers. The genetic map position is shown on the y-axis. Horizontal lines represent bins used as markers. Colored vertical lines show the physical position of each QTL for each trait in control conditions, salt conditions, or when STI values were mapped.

Supplemental Figures

Figure S1. Pearson correlations on raw phenotypes and transformed phenotypes for control and salt populations at 15 days and 45 days after treatment. (A) Control population 15 days after treatment (B) Salt population 15 days after treatment (C) Control population 45 days after treatment (D) Transformed control data 45 days after treatment (E) Salt population 45 days after treatment

Figure S2. Sorghum genetic map after using a sliding window method to call bin markers as AA (*S. propinquum*), BB (*S. bicolor*), or AB.

Figure S3. Sorghum genetic map after removing markers that deviated significantly from the expected mendelian ratio (1:1).

Figure S4. Final Sorghum genetic map used to map phenotypic traits after removing duplicate bins. Empty regions are regions that were removed because bins were either heterozygous, distorted, or were duplicates.

Tables

Table 1. Rank scoring parameters of plant vigor. Plant vigor was assessed on a scale of 0 to 5 with 0 indicating no signs of stress and 5 indicating plant death.

Score	Observation
0	No leaf signs
1	Some leaf and leaf tip curling
2	Severe leaf and leaf tip curling, few leaves elongated
3	Most leaves dead but still producing new leaves
4	*Plant still alive but no new growth*
5	Plant dead

Table 2. QTLs identified in the RIL population using transformed least square means in control conditions, salt conditions, and with stress tolerance index values. The QTLs reported were identified when using Multiple QTL Mapping (MQM) in control conditions (0 mM NaCl), salt conditions (75 mM NaCl), and with stress tolerance index (STI) values. QTLs are named using the following system: q[Trait][DAT]_[Chr].[Treatment]

Trait	Trt	QTL Name	DAT	Chr	Position (cM)	Bin (Max LOD)	Lod score	p-value	PVE	Additive	Start Mb	Peak Mb	End Mb
DAGB	Control	qDAGB45_2.C	45	2	52.64	56.26	3.33	1.02E-04	9.14	-0.06	13.85	56.26	58.70
DAGB	STI	qDAGB45_2.STI	45	2	52.64	56.26	4.42	7.53E-06	12.03	-0.17	13.85	56.26	56.74
HT	Control	qHT45_7.C	45	7	57.64	59.01	4.04	1.16E-04	9.64	-4.65	58.66	59.01	60.24
HT	Control	qHT45_9.C	45	9	64.00	55.07	4.75	2.35E-05	11.45	-5.19	54.37	55.07	56.91
HT	Salt	qHT45_1.S	45	1	125.00	77.03	4.93	1.58E-05	12.07	-4.36	18.46	77.03	80.57
HT	Salt	qHT45_7.S	45	7	63.29	60.17	4.13	9.52E-05	9.99	-3.86	59.01	60.17	61.46
HT	STI	qHT45_7.STI	45	7	58.80	59.35	3.80	1.99E-04	9.34	-0.04	58.68	59.35	60.24
HT	STI	qHT45_9.STI	45	9	64.00	55.07	3.61	3.00E-04	8.87	-0.04	54.37	55.07	56.68
LAGB	STI	qLAGB45_4.STI	45	4	73.00	66.68	6.26	1.30E-01	15.35	0.00	62.29	66.68	66.68
LAGB	STI	qLAGB45_5.STI	45	5	56.00	64.81	4.37	6.16E-02	10.40	0.00	6.15	64.81	66.57
RB	STI	qRB45_4.STI	45	4	67.00	62.29	3.29	1.12E-04	9.09	0.08	60.42	62.29	66.68
RS	STI	qRS45_7.STI	45	7	22.53	3.02	3.25	1.23E-04	9.00	-0.16	2.55	3.02	4.01
TAGB	STI	qTAGB45_4.STI	45	4	73.00	62.29	4.55	5.60E-06	12.34	0.12	62.17	62.29	66.68
TB	Salt	qTB45_4.S	45	4	73.00	62.29	4.90	1.67E-05	12.12	0.69	62.17	62.29	66.68
TB	Salt	qTB45_5.S	45	5	63.04	66.80	4.34	5.90E-05	10.64	0.39	64.50	66.80	67.30
TB	STI	qTB45_4.STI	45	4	71.00	62.29	4.82	2.97E-06	13.02	0.10	62.17	62.29	66.68

DAGB-dead aboveground biomass, LAGB-live aboveground biomass, RB-root biomass, RS-rank score, HT-height, TB-total biomass, TAGB-total aboveground biomass; Trt-treatment, STI-stress tolerance index, C-control, S-salt; P-*Sorghum propinquum*, B-*Sorghum bicolor*; DAT-days after treatment; Chr-chromosome, PVE-percent variance explained

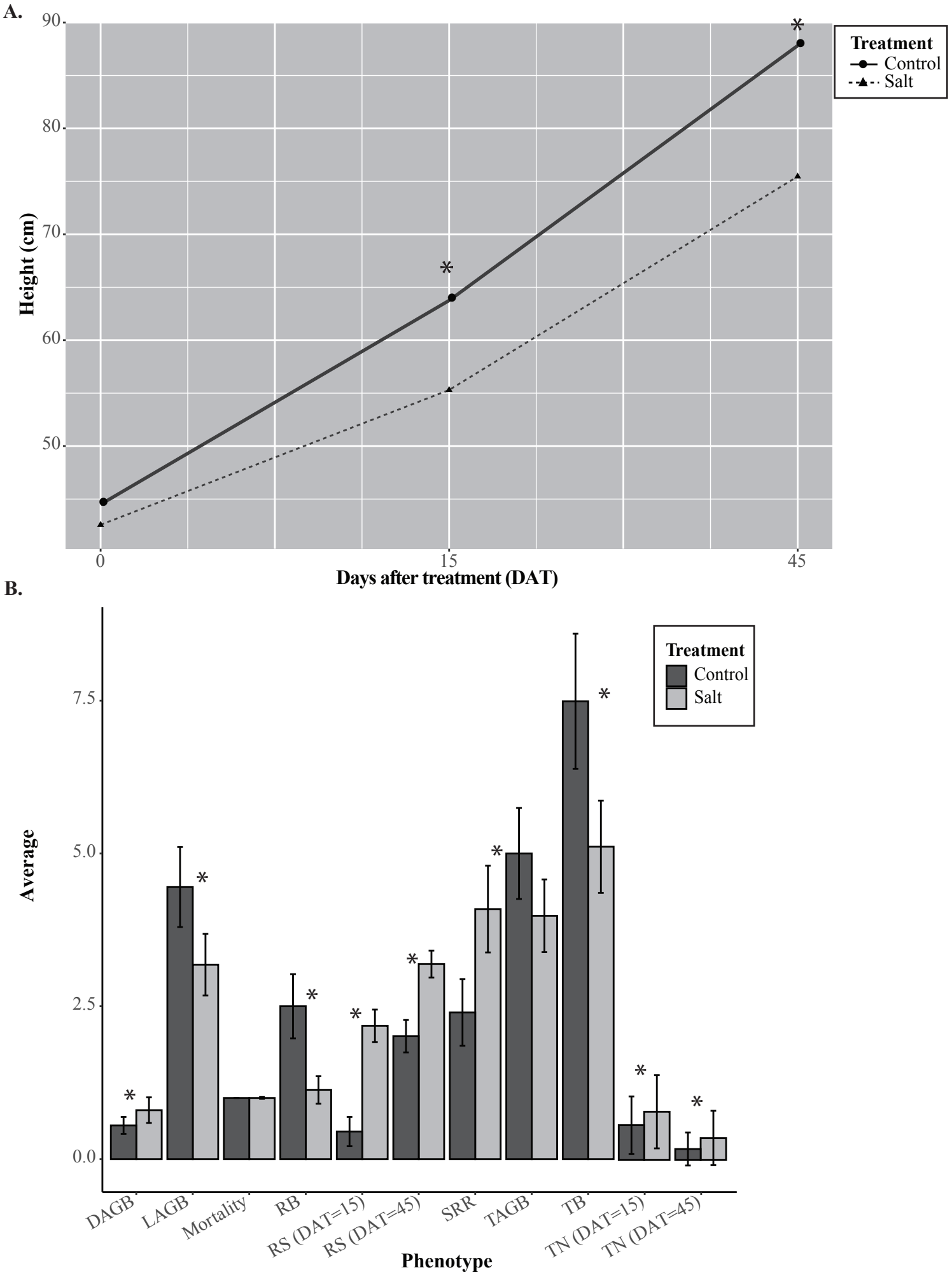

Figure 1 Phenotypic averages in control (0 mM NaCl) and treatment (75 mM NaCl) conditions.

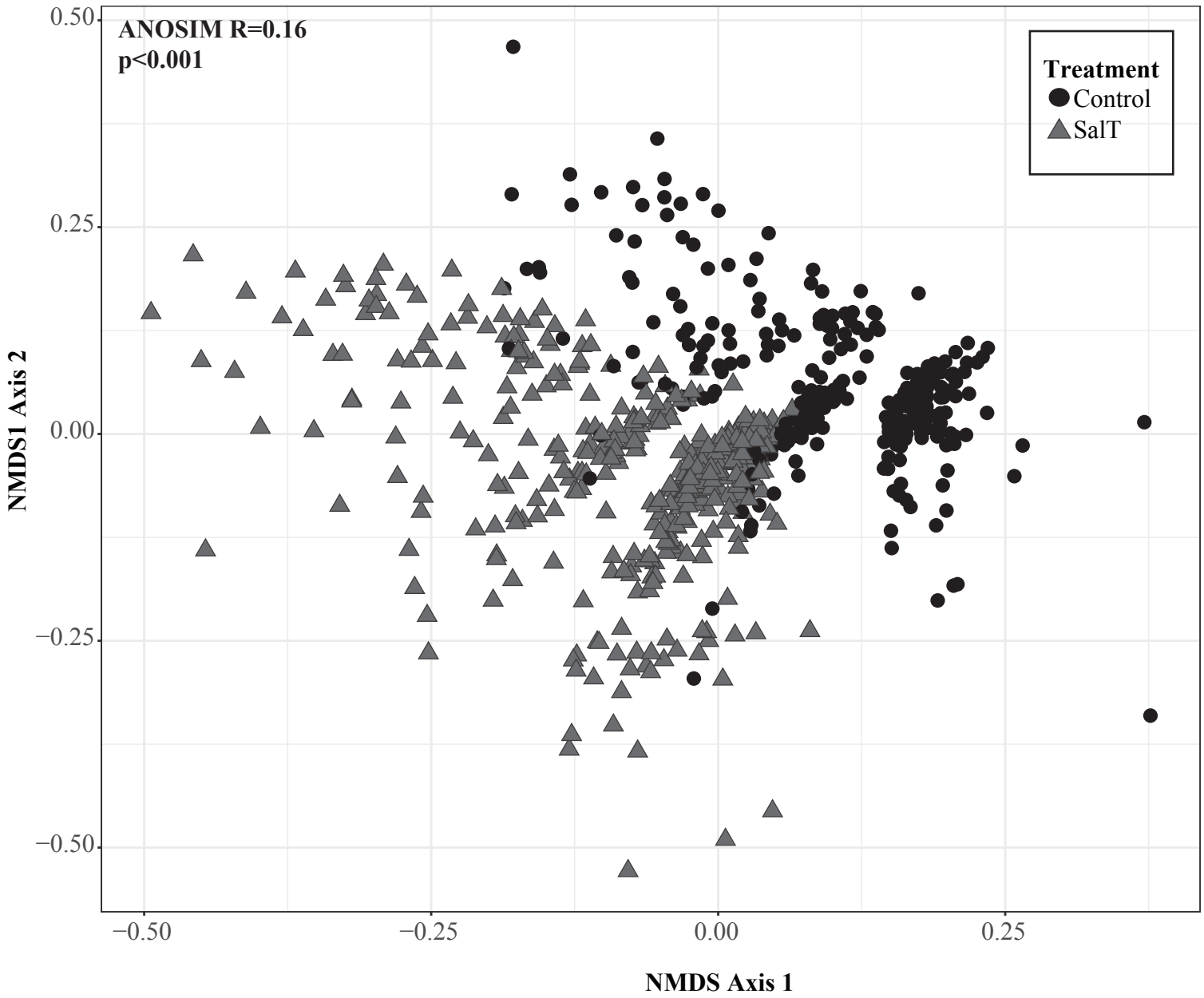

Figure 2. Non-metric multidimensional scaling (NMDS) analysis paired with an analysis of similarity (ANOSIM) reveals treatment clustering.

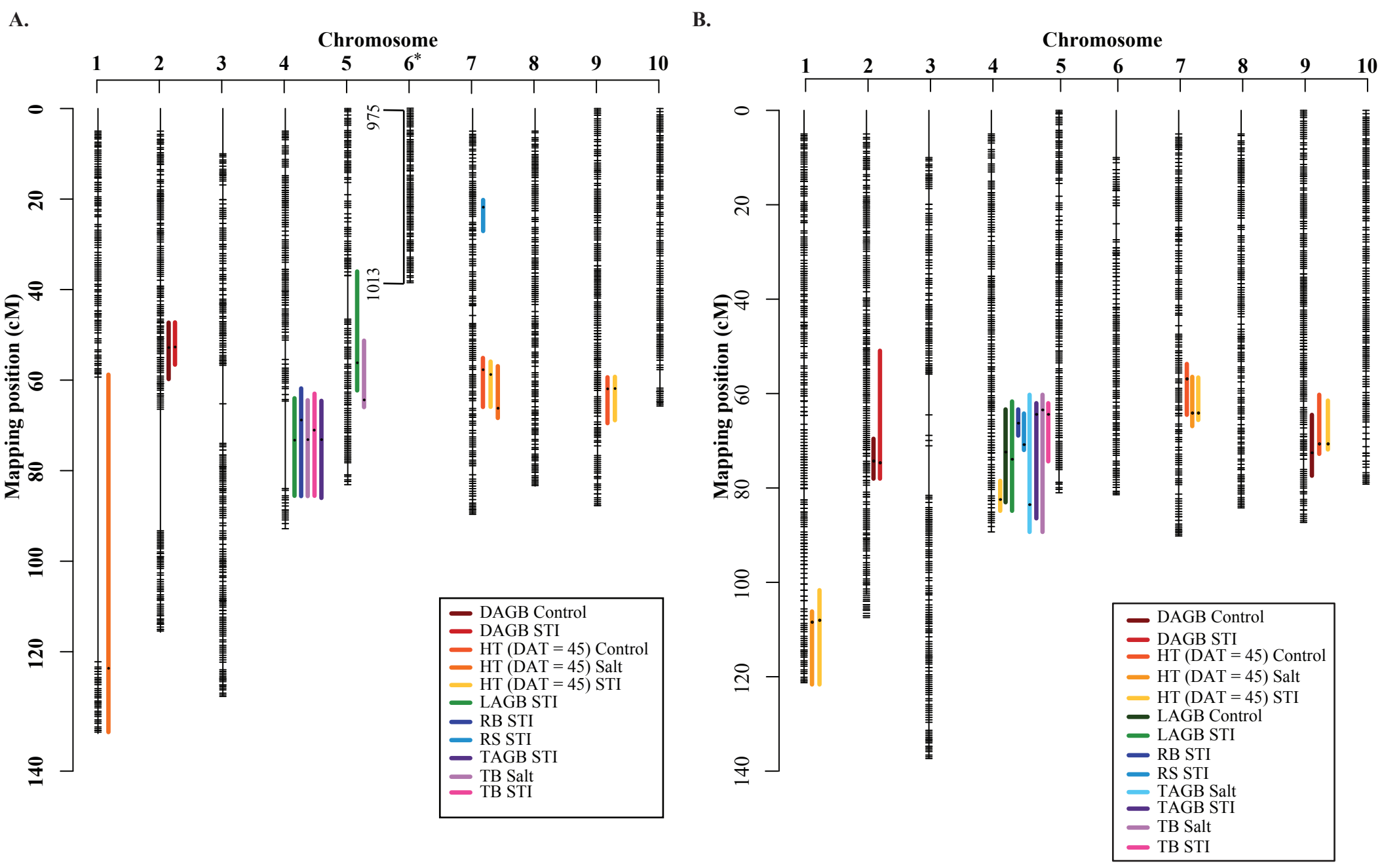

Figure 3. Sorghum genetic map with QTL locations for 14 traits from $177_{F3:F5}$ RILs.